Running Title: **Reticulons in primary plasmodesmata**

Author for correspondence: Prof. Karl Oparka
Regius Chair of Plant Science
Institute of Molecular Plant Science,
Rutherford Building,
University of Edinburgh,
Kings Buildings,
Mayfield Road,
Edinburgh
EH9 3BF
UK
karl.oparka@ed.ac.uk
+44 (0)131 650 7256

Research Area: Cell Biology

Putting the squeeze on PDs – a role for RETICULONS in primary plasmodesmata formation[1]

Kirsten Knox[2], Pengwei Wang[2#], Verena Kriechbaumer, Jens Tilsner, Lorenzo Frigerio, Imogen Sparkes, Chris Hawes and Karl Oparka*

Institute of Molecular Plant Sciences, University of Edinburgh, Edinburgh EH9 3BF United Kingdom (K.K., K.O.); Plant Cell Biology, Oxford Brookes University, Oxford, OX3 0BP, United Kingdom (V.K., P.W, C.H.); Biomedical Sciences Research Complex, University of St Andrews, St Andrews, KY16 9ST, United Kingdom (J.T); Life Sciences, University of Warwick, Coventry, CV4 7AL, United Kingdom (L.F.); Biosciences, College of Life and Environmental Sciences, Geoffrey Pope Building, University of Exeter, EX4 4QD United Kingdom (I.S).

Summary: Reticulon proteins involved in membrane curvature are targeted to the developing cell plate and label desmotubules in developing primary plasmodesmata

[1]This work was supported by grant BB/J004987/1 from the British Biotechnology and Biological Sciences Research Council (BBSRC) to K.O and C.H and by The Leverhulme Trust (F/00 382/G) to C.H.

[2] These authors contributed equally to the work.

[#] Current Address - School of Biological and Biomedical Sciences, Durham University, Durham, DH1 3LE, United Kingdom.

* Author for correspondence, karl.oparka@ed.ac.uk

Abstract

Primary plasmodesmata (PD) arise at cytokinesis when the new cell plate forms. During this process, fine strands of endoplasmic reticulum (ER) are laid down between enlarging Golgi-derived vesicles to form nascent PD, each pore containing a desmotubule, a membranous rod derived from the cortical ER. Little is known about the forces that model the ER during cell-plate formation. Here we show that members of the reticulon (RTNLB) family of ER-tubulating proteins may play a role in formation of the desmotubule. RTNLB3 and RTNLB6, two RTNLBs present in the PD proteome, are recruited to the cell plate at late telophase, when primary PD are formed, and remain associated with primary PD in the mature cell wall. Both RTNLBs showed significant co-localisation at PD with the viral movement protein of tobacco mosaic virus, while super-resolution imaging (3D-SIM) of primary PD revealed the central desmotubule to be labelled by RTNLB6. FRAP studies showed that these RTNLBs are mobile at the edge of the developing cell plate, where new wall materials are being delivered, but significantly less mobile at its centre where PD are forming. A truncated RTNLB3, unable to constrict the ER, was not recruited to the cell plate at cytokinesis. We discuss the potential roles of RTNLBs in desmotubule formation.

Introduction

Plasmodesmata (PD), the small pores that connect higher plant cells, are complex structures of about 50 nm in diameter. Each PD pore is lined by the plasma membrane and contains an axial ER-derived structure known as the desmotubule (Overall and Blackman, 1996; Maule, 2008; Tilsner et al., 2011). The desmotubule is an enigmatic structure whose function has not been fully elucidated. The small spiralling space between the desmotubule and the plasma membrane, known as the cytoplasmic sleeve, is almost certainly a conduit for movement of small molecules (Oparka et al., 1999). Some reports, however, suggest that the desmotubule may also function in cell-cell trafficking, providing an ER-derived pathway between cells along which macromolecules may diffuse (Cantrill et al., 1999). The desmotubule is one of the most tightly constricted membrane structures found in nature (Tilsner et al., 2011) but the forces that generate its intense curvature are not understood. In most PD, the desmotubule is a tightly furled tube of about 15 nm in diameter in which the membranes of the ER are in close contact along its length. The desmotubule may balloon out in the region of the middle lamella into a central cavity, but at the neck regions of the PD pore it is tightly constricted (Overall and Blackman, 1996; Ding et al., 1992; Ehlers and Kollmann, 2001; Glockmann and Kollmann, 1996; Robinson-Beers and Evert, 1991). Studies of PD using GFP targeted to the ER lumen (e.g. GFP-HDEL) have shown that GFP is excluded from the desmotubule due to the constriction of ER membranes in this structure (Oparka et al., 1999; Crawford and Zambryski, 2000; Martens et al., 2006; Guenoune-Gelbart et al., 2008). Lumenal GFP is therefore unable to move between plant cells unless the membranes of the desmotubule become 'relaxed' in some way. On the other hand, dyes and some proteins inserted into the ER membrane can apparently move through the desmotubule, either along the membrane or through the lumen, at least under some conditions (Grabski et al., 1993; Cantrill et al., 1999; Martens et al., 2006; Guenoune-Gelbart et al., 2008).

Recently, a number of proteins have been described in mammalian, yeast and plant systems that induce extreme membrane curvature. Among these are the RETICULONS (RTN), integral membrane proteins that induce curvature of the ER to

form tubules (Voeltz et al., 2006; Hu et al., 2008; Sparkes et al., 2010; Tolley et al., 2008; 2010). In animals, RTNs have been shown to be involved in a wide array of endomembrane related processes including intracellular transport, vesicle formation and as RTNs can also influence axonal growth, they may have roles in neuro-degenerative disorders such as Alzheimers (Yang and Strittmatter, 2007). Arabidopsis has 21 RTN homologs, known as RTNLBs (Nziengui et al., 2007; Sparkes et al., 2010), considerably more than in yeast or mammals, but most have not been examined. RTNLBs contain two unusually long hydrophobic helices that form re-entrant loops (Voeltz et al., 2006; Hu et al., 2008; Sparkes et al., 2010; Tolley et al., 2010). These are thought to induce membrane curvature by the molecular wedge principle (Hu et al., 2008; Shibata et al, 2009). When RTNLBs are overexpressed transiently in cells expressing GFP-HDEL, the ER becomes tightly constricted and GFP-HDEL is excluded from the lumen of the constricted ER tubules (Tolley et al., 2008; 2010), a situation similar to that which occurs in desmotubules (Oparka et al., 1999; Crawford and Zambryski, 2000; Martens et al., 2006). *In vitro* studies with isolated membranes have shown that the degree of tubulation is proportional to the number and spacing of RTNLB proteins in the membrane (Hu et al., 2008). For example, to constrict the ER membrane into a structure of 15 nm, the diameter of a desmotubule, would require RTNLBs to be inserted every 2 nm or less along the desmotubule axis (Hu et al., 2008), potentially making the desmotubule an extremely protein-rich structure (Tilney et al., 1991). Interestingly, a number of RTNLB proteins appear in the recently described PD proteome (Fernandez-Calvino et al., 2011) suggesting that RTNLBs are good candidates for proteins that model the cortical ER into desmotubules.

Primary PD form at cytokinesis during assembly of the cell plate (Hawes et al., 1981; Hepler, 1982). Of the numerous studies devoted to the structure of the cell plate, very few have examined the behaviour of the ER during cytokinesis. During mitosis, elements of ER are located in the spindle apparatus, separated from the cytoplasm (Hepler, 1980). Just prior to cytokinesis there is a relative paucity of ER in the region destined to become the cell plate (Hepler, 1980; Hawes et al. 1981). The studies of Hawes et al. (1981) and Hepler (1982), exploiting heavy-metal impregnation of the ER, showed that during the formation of the new cell plate strands of cortical ER are inserted across the developing wall, between the Golgi-derived vesicles that deposit

wall materials. These ER strands become increasingly thinner during formation of the desmotubule, eventually excluding heavy metal stains from the ER lumen (Hepler, 1982). The centre of the desmotubule often appears electron-opaque in TEM images and has been referred to as the 'central rod' (Overall and Blackman, 1996). This structure may consist of proteins that extend from the inner ER leaflets, or may correspond to head groups of the membrane lipids themselves. In the fully formed primary PD, the desmotubule remains continuous with the cortical ER that runs close to the new cell wall (Hawes et al., 1981; Hepler, 1982; Oparka et al., 1994).

Here we show that two of the RTNLBs present in the PD proteome, RTNLB3 and RTNLB6, become localised to the cell plate during the formation of primary PD. These RTNLBs remain associated with the desmotubule in fully formed PD and are immobile, as evidenced by FRAP studies. A truncated version of RTNLB3, in which the second hydrophobic region was deleted (Sparkes et al., 2010), was not recruited to the cell plate at cytokinesis. We suggest that RTNLBs play an important role in the formation of primary PD and discuss mechanisms by which these proteins may model the ER into desmotubules.

Results

RTNLBs appear at cell plates during cytokinesis

Of the 21 RTNLB homologs in the Arabidopsis database, we generated transgenic lines for RTNLBs 1-4 and 6, either as RTNLB-YFP or RTNLB-GFP fusions under CaMV 35S promoters. In all transgenic lines, RTNLBs labelled the ER in interphase cells (Fig. 1A-D). We noticed for some RTNLB lines that fluorescence became localised to the cell plate in dividing root cells. This localisation was recorded for RTNLBs 2, 3, 4 and 6 (Fig. 1E-H). In particular, strong cell-plate labelling was observed for RTNLB3 and RTNLB6 (Fig. 1G & H), two RTNLBs present in the PD proteome (Fernandez-Calvino et al., 2011).

To examine RTNLB distribution during cell division, we expressed Arabidopsis RTNLB3 and RTNLB6 in tobacco BY2 cells and followed their distribution in mitotically dividing cells. We used FM4-64 as a marker for the developing cell plate

(Bolte et al, 2004) and found that both RTNLBs showed strong co-localisation with FM4-64 labelled cell-plate membranes (Fig. 1I & J). We found a strong signal associated with the newly formed wall at the centre, and a more diffuse signal associated with the trailing edges of the cell plate (Fig. 1I & J). Next, we expressed the lumenal ER marker GFP-HDEL together with RTNLB3-YFP. In BY2 cells at interphase, as in Arabidopsis, GFP-HDEL is restricted to pockets in the ER by the RTNLB3-YFP mediated constriction of the ER lumen (Fig S1A). However, both RTNLB3-YFP and GFP-HDEL labelled the cortical ER uniformly throughout cell division (Fig. 1K & L). However, RTNLB3 became redistributed from the cortical ER into the developing cell plate during mid- and late-telophase, features not seen with GFP-HDEL (Fig. 1L). We next agro-infiltrated constructs of RTNLB3-YFP and RTNLB6-YFP into *Nicotiana benthamiana* plants transgenically expressing the movement protein of tobacco mosaic virus fused to GFP (TMV.MP-GFP; Oparka et al. 1999) that is known to locate to PD. In mature epidermal cells, we saw a significant co-localisation of these RTNLB-fusions with MP-GFP (Fig. 2).

Super-resolution imaging of primary PD

To confirm that RTNLBs were associated with desmotubules we used 3D-structured illumination microscopy (3D-SIM; see also Fitzgibbon et al., 2010) to examine primary PD in the walls between BY2 cells. To image the ER associated with PD more clearly, we plasmolysed adjacent cells expressing RTNLB3 or RTNLB6 and also imaged plasmolysed cells expressing RFP-HDEL for comparison. By confocal microscopy, we observed a strong RTNLB signal associated with punctae at the end walls of plasmolysed cells (Fig. 3A & B). Interestingly, Hechtian strands connecting the retracting protoplasts with the end walls showed strong RTNLB labelling, indicating that a constricted tubule of ER runs through each Hechtian strand (Fig. 3A & B). In contrast, we did not find RFP-HDEL within Hechtian strands or associated with PD (Fig. 3C), confirming previous reports that GFP targeted to the ER lumen is excluded from the centre of the desmotubule, where the ER membranes are in close contact (Oparka et al., 1999; Crawford and Zambryski, 2000; Martens et al., 2006; Guenoune-Gelbart et al., 2008). RFP-HDEL was also excluded from the Hechtian strands (Fig. 3C), indicating that during plasmolysis RFP-HDEL is ‘squeezed’ into the contracting protoplast.

With 3D-SIM we were able to resolve simple PD and found that desmotubules labelled with RTNLB6-GFP could be traced across individual cell walls (Fig. 3D-H). Often we observed the cortical ER undergoing abrupt changes in direction towards the entrance of a PD pore (Fig. 3G & H). Fig. 3J shows the cortical ER associated with a single post-division wall. Note that multiple ER strands extend from the adjoining cells and converge at the entrances of plasmodesmata where they can be traced across the wall. An enlargement of a region of cortical ER (Fig. 3I) shows that desmotubules are labelled with RTNLB6. A movie depicting the 3-dimensional arrangement of ER associated with PD is shown in supplementary movie 1. The optical sections shown in supplementary Fig. S2 were taken 150 nm apart in the axial dimension and show that a single RTNLB6-labelled desmotubule can be tracked as it crosses the cell wall.

FRAP reveals reduced RTNLB mobility during cell-plate formation

We used fluorescence recovery after photobleaching (FRAP) to study the mobility of RTNLBs in the developing cell plate. We compared the leading edge of the cell plate, where the RTNLB signal was diffuse (Fig. 4B) with the middle of the cell plate where RTNLB distribution was tightly confined (and where PD formation had presumably begun; Hawes et al., 1981, Hepler, 1982). We found a higher rate of fluorescence recovery at the edge of the cell plate compared to the centre, indicative of reduced RTNLB mobility during the formation of primary PD (Fig. 4A). At the completion of cytokinesis, we found that a strong RTNLB signal remained on the new cell wall (e.g. Fig. 1L). We then plasmolysed BY2 cells expressing RTNLB3 or RTNLB6 and performed FRAP on the ER associated with the primary PD in the cell wall. There was no fluorescence recovery in this location, although ER in the centre of the cell showed a characteristic fluorescence recovery (Fig. 4D). As BY2 cells often grow in linear chains, we also photobleached the ER of entire cells and monitored the bleached cell for fluorescence recovery. In this scenario, the only source of fluorescence is from neighbouring cells, across the intervening PD (see also Grabski et al., 1993). We failed to detect a return of fluorescence into the bleached cell, indicating that even though RTNLBs are present in the desmotubule, this structure does not form a conduit for RTNLB mobility between cells (Fig. 4E and F).

A RTNLB truncation is not recruited to the developing cell plate

Next, we utilised BY2 lines stably expressing a truncation of RTNLB3, comprising the first two trans-membrane domains and cytosolic loop, but lacking the c-terminal region predicted to form two transmembrane domains (RTNLB3t2; Sparkes et al, 2010). The ER in these cells was less tubular than in cells expressing the full length protein (Fig S1B). This truncated protein was not strongly recruited to the cell plate at cytokinesis and remained associated with the cytoplasmic ER (Fig. 5A and B). We then performed FRAP on cells expressing the RTNLB3t2. RTNLB3t2-YFP fluorescence in the cell plate of these cells recovered much more quickly than in those expressing the full-length RTNLB-YFP proteins (c.f. Fig. 5C with Fig. 4 A&B) and also at faster rates than lumenal GFP-HDEL (Fig. 5C).

Discussion

The desmotubule, the intercellular strand of cortical ER that runs through plasmodesmata, is an extremely constricted membrane tubule whose function remains unclear. Proteins of the reticulon family are candidates for shaping the desmotubule as they constrict ER membranes and appear in the Arabidopsis PD proteome (Fernandez-Calvino et al., 2011). Here we present data suggesting that reticulons are indeed involved in modelling the cortical ER into desmotubules during the formation of primary PD. Of the seven Arabidopsis RTNLBs analysed so far, none were localised exclusively to PD, although both RTNLB3 and RTNLB6 were significantly enriched at PD. The remainder were associated generally with the cortical ER (Nziengui et al., 2007; Tolley et al., 2008; 2010; Sparkes et al., 2010; this study). However, RTNLBs2-4 and RTNLB6 were recruited to the developing cell plate at cytokinesis, where substantial ER modifications occur during PD formation. Of these cell-plate localised reticulons, we focused on RTNLB3 and RTNLB6, both of which are present in the PD proteome (Fernandez-Calvino et al., 2011).

Our 3D-SIM data show that RTNLB6 remains associated with the highly constricted ER in primary PD of mature cell walls, and in Hechtian strands of plasmolysed cells. Both of these ER regions allow diffusion of the membrane dye $DiOC_6$ (Grabski et al., 1993; Oparka et al., 1994), but exclude lumenal GFP-HDEL (Oparka et al., 1999; Crawford and Zambryski, 2000; Martens et al., 2006; Guenoune-Gelbart et al., 2008). Tolley et al. (2008; 2010) showed that over-expression of RTNLB13 constricted the

cortical ER to an extent that lumenal GFP-HDEL was excluded, being forced into lumenal pockets distributed along tubules. Likewise the ER membrane marker GFP-calnexin demonstrated that tubular ER could be constricted to fine threads (Sparkes et al, 2010). Thus, there seems to be no *a priori* reason why RTNLBs could not form a structure similar to the desmotubule. However, since the RTNLBs are distributed over the entire cortical ER tubules, their presence alone cannot be sufficient to produce the strong constriction of the desmotubule.

The degree of membrane constriction produced by RTNs is dependent on their concentration (Hu et al., 2008). Our experiments provide no information on whether or not RTNLBs are enriched within PD. However, the ability of RTNLBs to constrict ER tubules depends on their oligomerisation, which in turn confers a loss of RTNLB mobility (Shibata et al., 2009; Tolley et al., 2010). Significantly, we observed reduced RTNLB3 and RTNLB6 mobility at the cell plate, and also in PD, as evidenced by FRAP analysis. Although RTNLB3 and RTNLB6 labelling was continuous between cells, no intercellular transport was detected, unlike that shown for the membrane dye $DiOC_6$ (Grabski et al., 1993) and the ER transmembrane proteins calnexin, and ACA2 (Guenoune-Gelbart et al., 2008). Truncated RTNLB3 (RTNLB3t2) in which the C-terminus proximal hydrophobic domain was deleted, a mutation that prevents oligomerisation and membrane constriction (Tolley et al., 2010; Sparkes et al., 2010), compromised recruitment to the cell plate and caused increased mobility on the plate ER. The mobility of RTNLB3t2 was in fact greater than free lumenal GFP, indicating that the hydrophobic domain of RTNLB3 is likely required for the formation of low-mobility oligomers (Tolley et al. 2010). Collectively, our data suggest that RTNLB3 and RTNLB6, and potentially other RTNLBs, oligomerise preferentially on those ER strands that traverse the cell plate during the formation of desmotubules. The positional cues that trigger this process remain unknown. RTNLBs1-7 form a cluster of closely related isoforms (Nziengui et al., 2007, Tolley et al., 2008) but their primary sequences contain no obvious clues as to why they should localise to the developing cell plate. It is likely that interactions with other proteins present at the cell plate and in PD may play a role in this context.

The desmotubule within PD often dilates in the middle lamella region of the wall, creating a central cavity whose function is unknown. *In vitro*, the linear spacing of

RTNs determines the degree of dilation between the RTN insertion points, the greater the distance between the constricting proteins the larger the membrane 'bulge' (Hu et al., 2008). Absence or removal of RTNLBs from the central cavity region of PD could provide a facile means of controlling ER dimensions within PD and may explain the dilation of the desmotubule in the central cavity. In the case of secondary PD, which form across already formed cell walls (Faulkner et al., 2008), RTNLBs may also play a role in ER modelling as the cortical ER strands on either sides of the wall must meet and fuse within secondary PD (Faulkner et al., 2008; Zhang & Hu, 2013).

In the electron microscope, globular proteins have been found along the length of the desmotubule, associated with the outer ER leaflet (Hepler, 1982; Ding et al., 1992; Ehlers and Kollmann, 2001). These have been suggested to be cytoskeletal elements (Overall and Blackman, 1996), but it is equally possible that they are proteins such as RTNLBs, responsible for maintaining the constriction of the desmotubule membranes and also linking the desmotubule to the PM (see also Tilsner et al., 2011). Several published electron micrographs show 'spoke-like' extensions between these proteins and the plasma membrane (Ding et al., 1992, Schulz, 1995, Overall and Blackman, 1996; Ehlers and Kollmann, 2001). These links with the plasma membrane, as well as other desmotubule-localised proteins, could contribute to a localised enrichment and immobilisation of RTNLBs. The extensive protein scaffold of the desmotubule is likely to impart considerable rigidity to this structure, and links to the plasma membrane would provide a means of exerting control of PD size exclusion limit (Tilsner et al., 2011). A schematic showing the putative distribution of RTNLB proteins on the desmotubule, and their links with the PM, is shown in Figure 6. We are currently searching for interactors of RTNLBs that may fulfil the above functions.

Many of the viral movement proteins that facilitate virus transport through PD interact with the cortical ER, or are integral ER membrane proteins (Vilar et al., 2002; Krishnamurthy et al., 2003; Martinez-Gil et al., 2009; Peiro et al., 2014). The transmembrane movement proteins of *Potato virus X* accumulate in RTNLB-rich regions of curved cortical ER in yeast (Wu et al., 2011) and also in the desmotubules of *Nicotiana benthamiana* PD (Tilsner et al., 2013). Viral movement proteins may disrupt the desmotubule scaffold by perturbing protein-lipid or protein-protein

interactions (Tilsner et al. 2011). The links between viral proteins and desmotubule proteins will be an interesting area for future research.

It remains to be shown how many of the RTNLB proteins in the Arabidopsis database are involved in membrane curvature alone, and RTNLBs may have additional functions at PD. A screen for proteins that interact with the FLAGELLIN SENSITIVE2 (FLS2) receptor identified RTNLB1 and RTNLB2 as interacting proteins, and these RTNLBs appear to regulate the transport of newly synthesised FLS2 from the ER to the plasma membrane (Lee et al., 2011). FLS2 is also enriched at PD (Faulkner et al., 2013). It will be interesting to determine whether other RTNLB members play roles in either intra- or inter-cellular signalling.

Materials and Methods

Plant material

Arabidopsis seeds were sterilised with 10% (v/v) bleach, rinsed once in 70% (v/v) ethanol and then rinsed four times in sterile ddH_2O. Unless otherwise stated seeds were plated in petri dishes on Murashige and Skoog medium with 1% sucrose (w/v), solidified with 1.2% (w/v) phytoagar and grown in 16-h photoperiods with 200 μE m^{-2} s^{-1} at 18°C to 22°C.

Molecular Biology and cloning

The generation of both the RTNLB-YFP and the RTNLB3 truncation constructs have previously been described (Sparkes et al 2010). RTNLB3 and RTNLB6 were amplified by PCR from ABRC clones (ABRC), recombined into Gateway vector pDONR201, and then both were recombined into binary vector pGWB405 creating c-terminal GFP fusions (Nakagawi et al, 2007). All binary vectors were then transformed into *Agrobacterium tumefaciens* GV3101 and thence into Arabidopsis (Col-0) using the floral dip method (Clough & Bent, 1998).

BY2 cell culture and transformation

Tobacco BY2 cells (*Nicotiana tabacum* cv BY-2 [Bright Yellow 2]) cell lines (Nagata et al, 1992) were cultured aseptically in liquid media containing 4.3 g l^{-1} Murashige and Skoog Basal Media (Sigma, M5519), 200 µg ml^{-1} 2,4-Dichlorophenoxyacetic acid and 30 g l^{-1} sucrose. Cells were grown in the dark at 28°C on an orbital shaker and sub-cultured to fresh media weekly. RTNLB3-GFP and RTNLB6-GFP transgenic lines were generated by *Agrobacterium tumefaciens* mediated transformation with the binary vectors described above. 40µl of 20 mM acetosyringone was added to 40ml of 3 day old BY2 cell culture and cells were pipetted up and down 20 times to induce minor cell damage. The cells were then mixed with 100µl of the appropriate agrobacterium overnight culture and incubated at 28°C in the dark for 3 days. Cells were then washed 3 times in sterile media, resuspended in 5ml and plated on media solidified with 0.75% (w/v) phytoagar with 50µg ml^{-1} cefotaxime and 50µg ml^{-1} kanamycin. Plates were incubated for 3-4 weeks. Resultant calli were then sub-cultured onto fresh selective media to confirm antibiotic resistance before expression was assessed under fluorescence microscope and positive cell lines transferred and maintained in liquid culture. Cells were imaged at day 4 post sub-culture for cell plate studies and plasmolysis and day 4-6 for FRAP.

Confocal imaging and cell staining

Seedlings and BY2 cells were imaged live on slides using either a Leica SP2 Confocal Laser-Scanning Microscope (Leica Microsystems) with 40x and 63x water-immersion lens (HCX PLAPO CS; Leica Microsystems) or a Zeiss LSM510 Meta laser scanning confocal microscope with 40x or 63x oil immersion objectives. For cell plate images 3-day old Arabidopsis seedlings were partially synchronised by transferring to media containing 2 mM Hydroxyurea for 15-17 hours before imaging the roots. Arabidopsis roots were stained with 10µg ml^{-1} propidium iodide, where indiciated. BY2 cells were stained with 8.5 µg ml-1 Calcafluor White for 1h or 2 µM

FM4-64 (Synaptored) for 10 minutes and then media removed and replaced with fresh before imaging or plasmolysis.

Plasmolysis experiments

BY2 cells were plasmolysed in a 0.45 M solution of Mannitol in liquid BY2 media for 20 minutes, then mounted on slides in the osmoticum to maintain plasmolysis throughout imaging.

Fluorescence Recovery after Photobleaching (FRAP)

FRAP analyses were conducted either on a a Zeiss LSM510 Meta Confocal Laser-Scanning Microscope (Zeiss) or a Leica SP2 Confocal Laser-Scanning Microscope (Leica Microsystems) under the 63x objective using rapid switching between low intensity imaging and high intensity bleach mode. Pre and post bleach images were collected using 40% intensity of the 488 laser. Bleaching of the selected region, either an entire cell, a cell wall or square regions of interest (ROIs) on the middle or edges of cell plates, was achieved with 5-10 scans at 100% intensity of the 488nm laser. Subsequent recovery was monitored for up to 5 minutes, dependent on experiment. Relative levels of fluorescence were normalised to the first post-bleach reading. Data are the mean of at least 9 replicates with bars indicating the standard error of the mean (SEM).

3D-SIM Microscopy

3D-SIM microscopy is fully described in Fitzgibbon et al., (2010) Briefly, the 3D-SIM images were obtained using a Deltavision OMX Blaze microscope (GE Healthcare) equipped with 405, 488 and 593 nm solid state lasers and a UPlanSApochromat 100x 1.4 numerical aperture oil immersion objective (Olympus). To maintain the delicate ER structure, BY2 cells were imaged live. Exposure times

were typically between 100 and 200 ms, and the power of each laser was adjusted to achieve optimal intensities of between 1,000 and 3,000 counts in a raw image of 15-bit dynamic range of Edge sCMOS camera (PCO AG, Germany). As photobleaching of the GFP was an issue in the live cells, exposure times and laser power were adjusted to minimal levels. Unprocessed image stacks were composed of 15 images per z-section (five phase-shifted images per each of three interference pattern angles). Super-resolution three-dimensional image stacks were reconstructed with SoftWoRx 6.0 (GE) using channel specific OTFs and Wiener filter setting of 0.002 (0.005 for the DAPI channel) to generate a super-resolution three-dimensional image stack. Images from the different colour channels, recorded on separate cameras, were registered with SoftWorx 6.0 alignment tool (GE).

Accession Numbers

Sequence data for genes in this article can be found in GenBank/EMBL databases using the following accession numbers: RTNLB1, At4g23630; RTNLB2, At4g11220; RTNLB3, At1g64090; RTNLB4, At5g41600 and RTNLB6, At3g61560.

Acknowledgements

We are grateful for the technical expertise and assistance of Dr Markus Posch at the OMX facility, University of Dundee. Use of the OMX microscope was supported by an MRC Next Generational Optical Microscopy Award (MR/K015869/1).

Author Contributions

K.K, V.K, J.T, C.H and K.O designed research. K.K, P.W, V.K, J.T. L.F and I.S performed the research. K.K, P.W, V.K, C.H and K.O analysed the data. K.K, K.O wrote the paper.

Figure Legends

Figure 1

RETICULON localisation in Arabidopsis and Tobacco BY2 cells. RTNLBs label the ER but not the nuclear envelope in Arabidopsis leaf epidermis. **A**, RTNLB1-YFP **B**, RTNLB2-YFP **C**, RTNLB3-GFP **D**, RTNLB6-GFP. RTNLBs are recruited to the developing cell plate in Arabidopsis root cells **E**, RTNLB2-YFP **F**, RTNLB4-YFP **G**, RTNLB3-GFP **H**, RTNLB6-GFP. RTNLB3-GFP (**I**) and RTNLB6-GFP (**J**) are also recruited to the cell plate in BY2 cells. FM4-64 (red) strongly labels the cell plate. Overlaid images show that the RTNLB-GFP signal is more diffuse at the edges of the developing cell plate. RTNLB is recruited specifically from the cortical ER to the developing cell plate. During early telophase (**K**) RTNLB3-YFP and GFP-HDEL label both the cortical ER and the cell plate but by late telophase (**L**) RTNLB3 becomes redistributed into the cell plate. Bars = 5 μm.

Figure 2

Co-localisation of the movement protein of tobacco mosaic virus (MP-GFP; green) with RTNLB3-YFP (**A**) and RTNLB6-YFP (**B**; magenta). Plasmodesmata showing co-localisation signals appear white.

Figure 3

RTNLBs label the Hechtian strands of plasmolysed BY2 cells and show continuous labelling through PD. **A** and **B**, confocal images of RTNLB3-GFP (**A**) or RTNLB6-GFP (**B**) labelling of the Hechtian strands (green) in a plasmolysed BY2 cell. Calcofluor (blue) was used to visualise the cell wall between plasmolysed cells. GFP-labelled punctae were observed along the adjoining cell wall (darts), indicating the positions of PD. **C**, RFP-HDEL does not reveal the Hechtian strands or PD, leaving the space between the plasma membrane and cell wall unlabelled (*). **D-J**, 3D-SIM images of plasmolysed BY2 cells expressing RTNLB6-GFP. **D-F** RTNLB6-GFP labelled ER in Hechtian strands is severely constricted as it passes through PD. **E** and **F**, close up of boxed area in **D**, darts indicate areas of highly constricted ER, forming the desmotubule at the core of PD. **G** and **H**, the cortical ER shows abrupt changes in direction towards the entrance to a PD (*). **I**, single-channel close up of boxed region

in **J**, showing the extreme constriction of the labelled ER. **J**, a section of the cell wall between cells (blue dashed line) showing that the RTNLB6-GFP labelled ER is continuous across the cell wall. Bars = 5 μm (A-C); 1 μm (D-I) and 0.5 μm (F).

Figure 4

Fluorescence recovery after photobleaching (FRAP) reveals that RTNLB mobility is reduced in areas of PD development during cell plate formation.

A, FRAP comparing the leading edge of the developing cell plate (light and dark blue) with the centre of the cell plate (black diamonds) in BY2 cells expressing RTNLB3-YFP. B shows representative pre- and post-bleach images. Boxes indicate the bleached regions. C, RTNLB6-GFP on the ER associated with the primary PD at the cell wall in plasmolysed BY2 cells is immobile (blue diamonds), whereas within the protoplast, fluorescence recovers (red triangles) indicating RTNLB6-GFP mobility. D shows representative pre- and post-bleach images of RTNLB6-GFP labelled plasmolysed BY2 cells. Boxes indicate the bleached regions. E, whole cells bleached within a chain show that RTNLBs are not mobile between cells. F shows representative pre- and post-bleach images of RTNLB6-GFP labelled BY2 cells. Boxes indicate the bleached cell. Data are averages of at least 9 separate experiments and bars indicate standard error of the mean (SEM). Bars = 5 μm.

Figure 5

A truncated version of RTNLB3 (RTNLB3t2) is not recruited to the cell plate. **A** and **B** show RTNLB3t2-YFP co-expressed with GFP-HDEL. The overlaid images show that the RTNLB3t2 has even distribution across the ER, identical to GFP-HDEL, with no specific recruitment to the cell plate. **C**, FRAP of the cell plate in cells expressing RTNLB3t2-YFP showing that fluorescence recovers rapidly in the cell plate compared to GFP-HDEL and intact RTNLB3 (**D**, c.f. Fig.4 **A**). **D** and **E** representative pre- and post-bleach images. Bars = 5 μm.

Figure 6

Model showing the insertion of RTNLB proteins into the membranes of the desmotubule. Putative protein-protein interactions between RTNLBs and proteins resident in the plasma membrane are depicted as broken lines.

Literature Cited

Bolte S, Talbot C, Boutte Y, Catrice O, Read ND, Satiat-Jeunemaitre B (2004) FM-dyes as experimental probes for dissecting vesicle trafficking in living plant cells. J Microscopy **214**(2):159-173

Cantrill LC, Overall RL, Goodwin PB (1999) Cell-to-cell communication via plant endomembranes. Cell Biol Int **23**:653–661

Clough SJ, Bent AF (1998) Floral dip: A simplified method for Agrobacterium-mediated transformation of Arabidopsis thaliana. Plant J **16**(6):735-43

Crawford KM, Zambryski PC (2000) Subcellular localization determines the availability of non-targeted proteins to plasmodesmatal transport. Curr Biol **10**:1032–1040

Ding B, Turgeon R, Parthasarathy MV (1992) Substructure of freeze-substituted plasmodesmata. Protoplasma **169**:28–41

Ehlers K, Kollmann R (2001) Primary and secondary plasmodesmata: structure, origin and functioning. Protoplasma **216**:1–30

Faulkner C, Akman OE, Bell K, Jeffree C, Oparka K (2008) Peeking into pit fields: a multiple twinning model of secondary plasmodesmata formation in tobacco. Plant Cell **20**:1504–1518

Faulkner C, **Petutschnig E, Benitez-Alfonso Y, Beck M, Robatzek S, Lipka V, Maule AJ** (2013) LYM2-dependent chitin perception limits molecular flux via plasmodesmata. Proc Natl Acad Sci USA **110**(22):9166-70

Fernandez-Calvino L, Faulkner C, Walshaw J, Saalbach G, Bayer E, Benitez-Alfonso Y, Maule A (2011) Arabidopsis plasmodesmal proteome. PLoS One **6**(4):e18880

Fitzgibbon J, Bell K, King E, Oparka K (2010) Super-resolution imaging of plasmodesmata using three-dimensional structured illumination microscopy. Plant Physiol **153**(4):1453-63

Glockmann C, Kollmann R (1996) Structure and development of cell connections in the phloem of *Metasequoia glyptostroboides* needles I. Ultrastructural aspects of modified primary plasmodesmata in Strasburger cells. Protoplasma **193**:191–203

Grabski S, de Feijter AW, Schindler M (1993) Endoplasmic reticulum forms a dynamic continuum for lipid diffusion between contiguous soybean root cells. Plant Cell **5**:25–38

Guenoune-Gelbart D, Elbaum M, Sagi G, Levy A, Epel BL (2008) Tobacco mosaic virus (TMV) replicase and movement protein function synergistically in facilitating tmv spread by lateral diffusion in the plasmodesmal desmotubule of *Nicotiana benthamiana*. Mol Plant Microb Interact **21**:335–345

Hawes CR, Juniper BE, Horne JC (1981) Low and high voltage electron microscopy of mitosis and cytokinesis in maize roots. Planta **152**:397–407

Hepler PK (1980) Membranes in the mitotic apparatus of barley cells. J Cell Biol **86**(2):490-9

Hepler PK (1982) Endoplasmic reticulum in the formation of the cell plate and plasmodesmata. Protoplasma **111**:121–133

Hu J, Shibata Y, Voss C, Shemesh T, Li Z, Coughlin M, Kozlov MM, Rapoport TA, Prinz WA (2008) Membrane proteins of the endoplasmic reticulum induce high-curvature tubules. Science **319**:1247–1250

Krishnamurty K, Heppler M, Mitra R, Blancaflor E, Payton M, Nelson RS, Verchot-Lubicz J (2003) The *Potato virus X* TGBp3 protein associates with the ER network for virus cell-to-cell movement. Virology **309**:269–281

Lee HY, Bowen CH, Popescu GV, Kang HG, Kato N, Ma S, Dinesh-Kumar S, Snyder M, Popescu SC (2011) Arabidopsis RTNLBLB1 and RTNLBLB2 reticulon-like proteins regulate intracellular trafficking and activity of the FLS2 immune receptor. Plant Cell **23**(9):3374-91

Martínez-Gil L, Sanchez-Navarro JA, Cruz A, Pallas V, Perez-Gil J, Mingarro I (2009) Plant virus cell-to-cell movement is not dependent on the transmembrane disposition of its movement protein. J Virol **83**:5535–5543

Maule AJ (2008) Plasmodesmata: structure, function and biogenesis. Curr Opin Plant Biol **11**:680–686

Martens HJ, Roberts AG, Oparka KJ, Schulz A (2006) Quantification of plasmodesmatal endoplasmic reticulum coupling between sieve elements and companion cells using fluorescence redistribution after photobleaching. Plant Physiol **142**:471–480

Nagata T, Nemoto Y, Hasezawa S (1992) Tobacco BY-2 cell line as the "He-La" cell in the cell biology of higher plants. Int Rev Cyt **132**:1-30

Nakagawa T, Kurose T, Hino T, Tanaka K, Kawamukai M, Niwa Y, Toyooka K, Matsuoka K, Jinbo T and Kimura T (2007) Development of series of gateway binary vectors, pGWBs, for realizing efficient construction of fusion genes for plant transformation. J Biosci Bioeng **104**(1):34-41

Nziengui H, Bouhidel K, Pillon D, Der C, Marty F, Schoefs B (2007) Reticulon-like proteins in *Arabidopsis thaliana*: structural organization and ER localization. FEBS Lett **581**:3356–3362

Oparka KJ, Prior DAM, Crawford JW (1994) Behavior of plasma-membrane, cortical ER and plasmodesmata during plasmolysis of onion epidermal-cells. Plant Cell Environ **17**:163–171

Oparka KJ, Roberts AG, Boevink P, Santa Cruz S, Roberts IM, Pradel KS, Imlau A, Kotlizky G, Sauer N, Epel BL (1999) Simple, but not branched, plasmodesmata allow the nonspecific trafficking of proteins in developing tobacco leaves. **Cell** 97:743–754

Overall RL, Blackman LM (1996) A model of the macro-molecular structure of plasmodesmata. Trends Plant Sci **1**:307–311

Peiro A, Martinez-Gil L, Tamborero S, Pallas V, Sanchez-Navarro JA, Mingarro I (2014) The tobacco mosaic virus movement protein associates with but does not integrate into biological membranes. J Virol **88**(5):3016-26

Robinson-Beers K, Evert RF (1991) Fine structure of plasmodesmata in mature leaves of sugarcane. Planta **184**:307–318

Schulz A (1995) Plasmodesmal widening accompanies the short-term increase in symplasmic phloem unloading in pea root-tips under osmotic stress. Protoplasma **188**: 22–37

Shibata Y, Hu J, Kozlov MM, Rapoport TA (2009) Mechanisms shaping the membranes of cellular organelles. Annu Rev Cell Dev Biol **25**:329-54

Sparkes IA, Tolley N, Aller I, Svozil J, Osterrieder A, Botchway S, Mueller C, Frigerio L, Hawes C (2010) Five arabidopsis reticulon isoforms share endoplasmic reticulum location, topology, and membrane-shaping properties. Plant Cell **22**:1333–1343

Tilney LG, Cooke TJ, Connelly PS, Tilney MS (1991) The structure of plasmodesmata as revealed by plasmolysis, detergent extraction, and protease digestion. J Cell Biol **112**:739–747

Tilsner J, Amari K, Torrance, L (2011) Plasmodesmata viewed as specialized membrane adhesion sites. Protoplasma **248** (1): 39-60

Tilsner J, Linnik O, Louveaux M, Roberts IM, Chapman SN, Oparka KJ (2013) Replication and trafficking of a plant virus are coupled at the entrances of plasmodesmata. J Cell Biol **201**(7):981-95

Tolley N, Sparkes IA, Hunter PR, Craddock CP, Nuttall J, Roberts LM, Hawes C, Pedrazzini E, Frigerio L (2008) Overexpression of a plant reticulon remodels the lumen of the cortical endoplasmic reticulum but does not perturb protein transport. Traffic **8**:94–102

Tolley N, Sparkes I, Craddock CP, Eastmond PJ, Runions J, Hawes C, Frigerio L (2010) Transmembrane domain length is responsible for the ability of a plant reticulon to shape endoplasmic reticulum tubules in vivo. Plant J **64**(3):411-8

Vilar M, Sauri A, Monne M, Marcos JF, von Heijne G, Perez-Paya E, Mingarro I (2002) Insertion and topology of a plant viral movement protein in the endoplasmic reticulum membrane. J Biol Chem **277**(26):23447-52

Voeltz GK, Prinz WA, Shibata Y, Rist JM, Rapoport TA (2006) A class of membrane proteins shaping the tubular endoplasmic reticulum. Cell **124**:573–586

Wu ZY, Lee SC, Wang CW (2011) Viral protein targeting to the cortical endoplasmic reticulum is required for cell-cell spreading in plants. J Cell Biol 193(3):521-35

Yang YS, Strittmatter SM (2007) The reticulons: a family of proteins with diverse functions. Genome Biol **8**(12): 234

Zhang M, Hu J (2013) Homotypic fusion of endoplasmic reticulum membranes in plant cells. Front plant Sci **18**(4):514

Figure 1

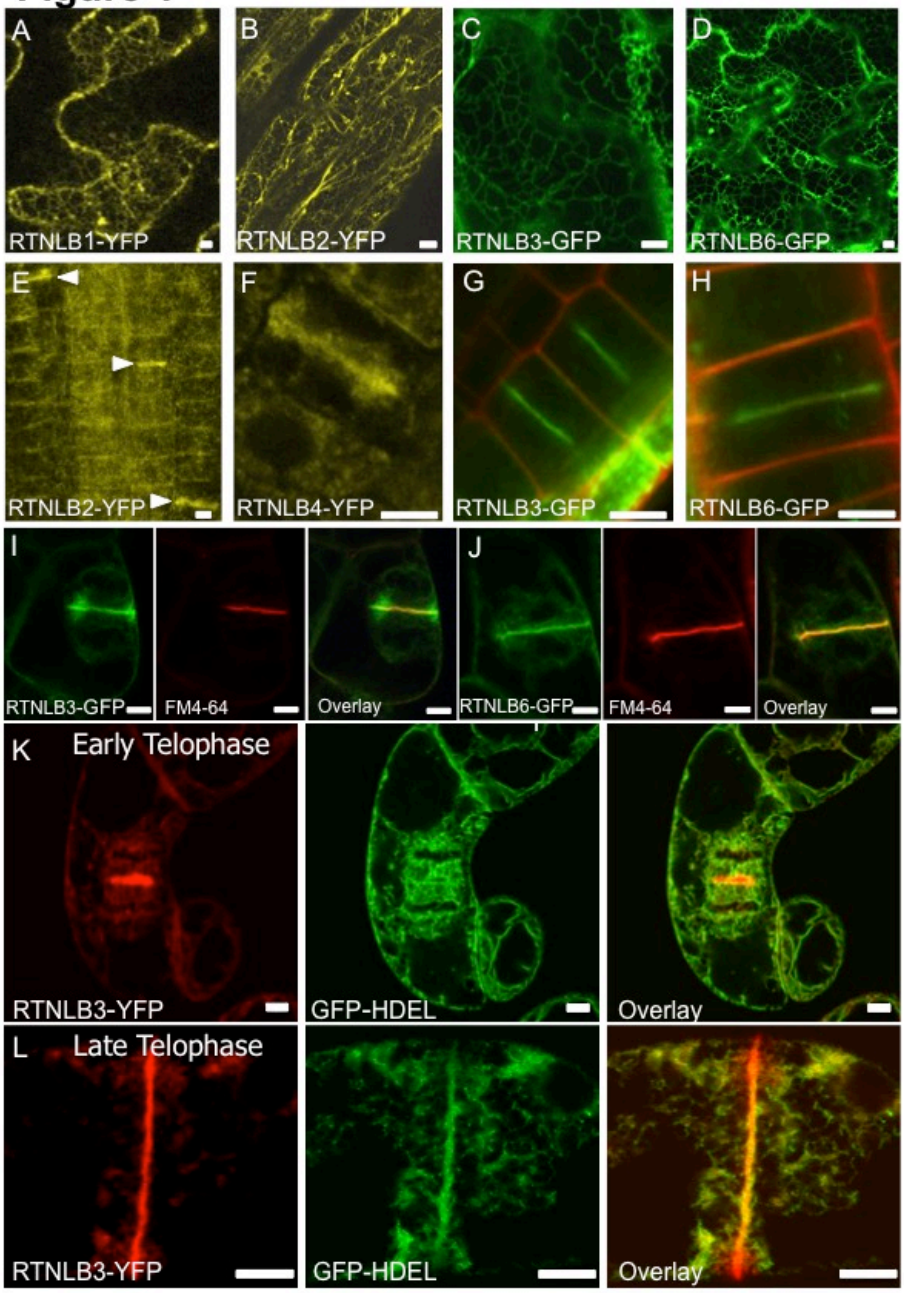

Figure 1
RETICULON localisation in Arabidopsis and Tobacco BY2 cells. RTNLBs label the ER but not the nuclear envelope in Arabidopsis leaf epidermis. **A**, RTNLB1-YFP **B**, RTNLB2-YFP **C**, RTNLB3-GFP **D**, RTNLB6-GFP. RTNLBs are recruited to the developing cell plate in Arabidopsis root cells **E**, RTNLB2-YFP **F**, RTNLB4-YFP **G**, RTNLB3-GFP **H**, RTNLB6-GFP. RTNLB3-GFP (**I**) and RTNLB6-GFP (**J**) are also recruited to the cell plate in BY2 cells. FM4-64 (red) strongly labels the cell plate. Overlaid images show that the RTNLB-GFP signal is more diffuse at the edges of the developing cell plate. RTNLB is recruited specifically from the cortical ER to the developing cell plate. During early telophase (**K**) RTNLB3-YFP and GFP-HDEL label both the cortical ER and the cell plate but by late telophase (**L**) RTNLB3 becomes redistributed into the cell plate. Bars = 5 μm.

Figure 2

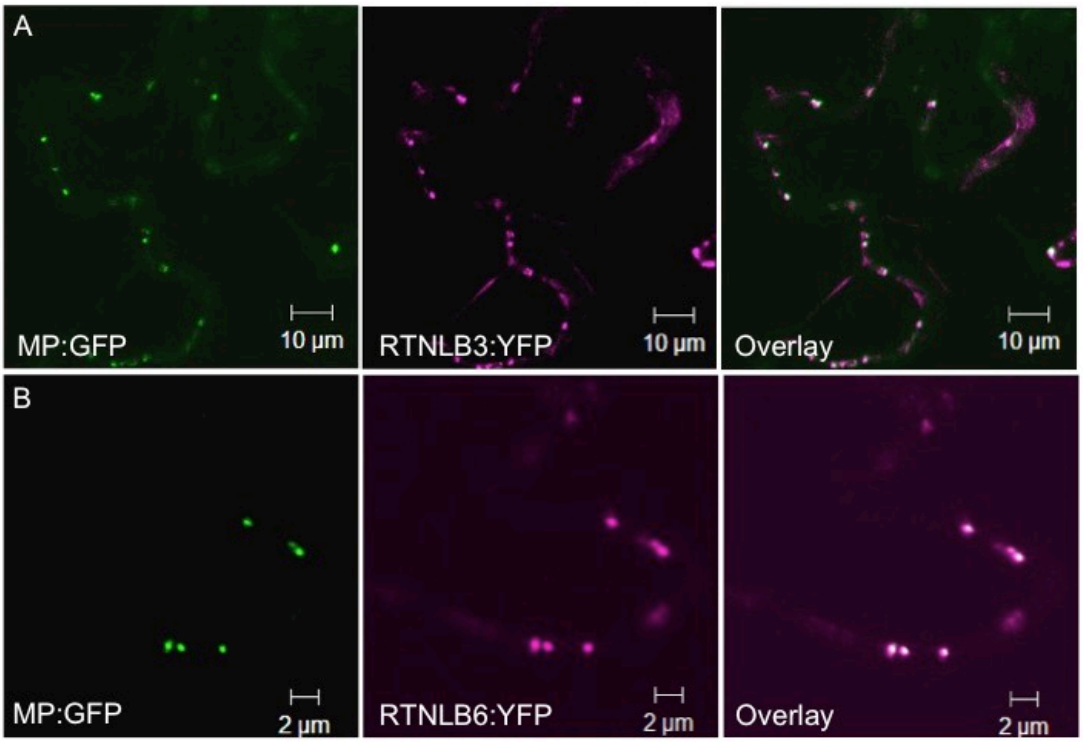

Figure 2
Co-localisation of the movement protein of tobacco mosaic virus (MP-GFP; green) with RTNLB3-YFP (**A**) and RTNLB6-YFP (**B**; magenta). Plasmodesmata showing co-localisation signals appear white.

Figure 3

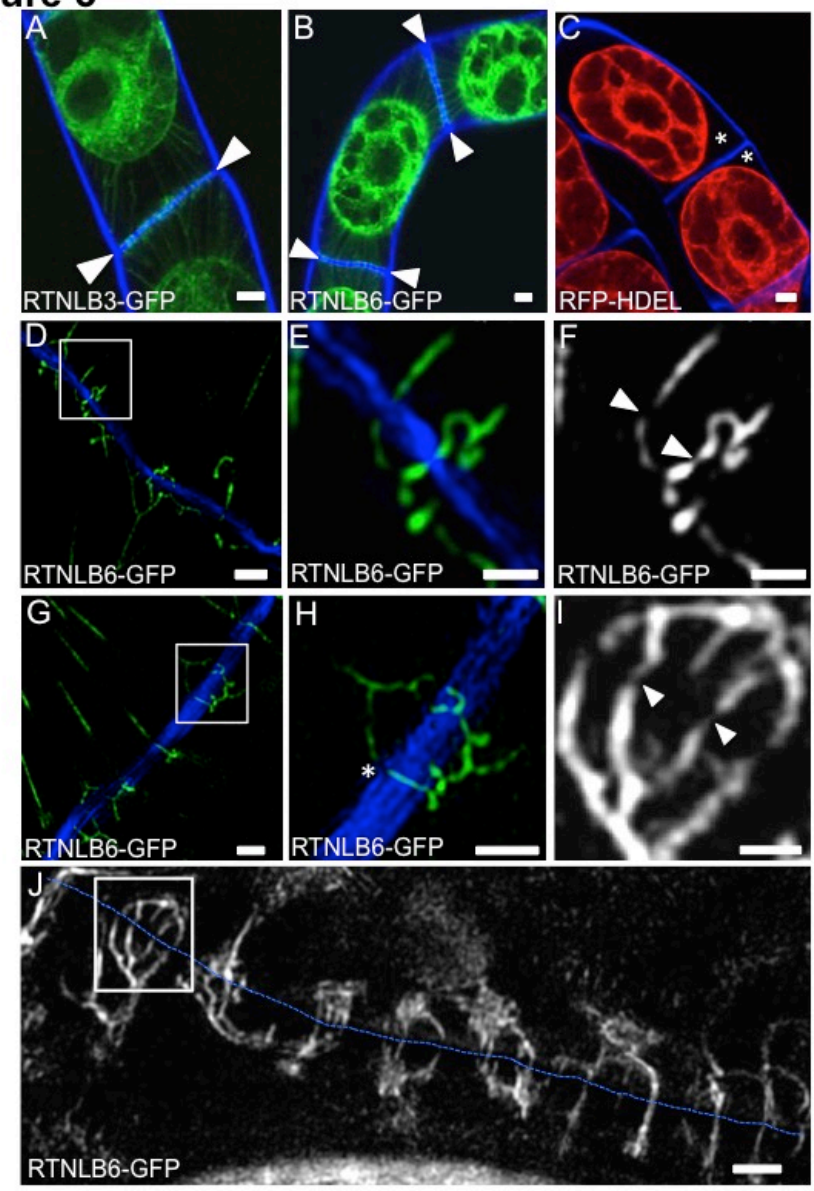

Figure 3

RTNLBs label the Hechtian strands of plasmolysed BY2 cells and show continuous labelling through PD. **A** and **B**, confocal images of RTNLB3-GFP (**A**) or RTNLB6-GFP (**B**) labelling of the Hechtian strands (green) in a plasmolysed BY2 cell. Calcofluor (blue) was used to visualise the cell wall between plasmolysed cells. GFP-labelled punctae were observed along the adjoining cell wall (darts), indicating the positions of PD. **C**, RFP-HDEL does not reveal the Hechtian strands or PD, leaving the space between the plasma membrane and cell wall unlabelled (*). **D-J**, 3D-SIM images of plasmolysed BY2 cells expressing RTNLB6-GFP. **D-F** RTNLB6-GFP labelled ER in Hechtian strands is severely constricted as it passes through PD. **E** and **F**, close up of boxed area in **D**, darts indicate areas of highly constricted ER, forming the desmotubule at the core of PD. **G** and **H**, the cortical ER shows abrupt changes in direction towards the entrance to a PD (*). **I**, single-channel close up of boxed region in **J**, showing the extreme constriction of the labelled ER. **J**, a section of the cell wall between cells (blue dashed line) showing that the RTNLB6-GFP labelled ER is continuous across the cell wall. Bars = 5 µm (A-C); 1 µm (D-I) and 0.5 µm (F).

Figure 4

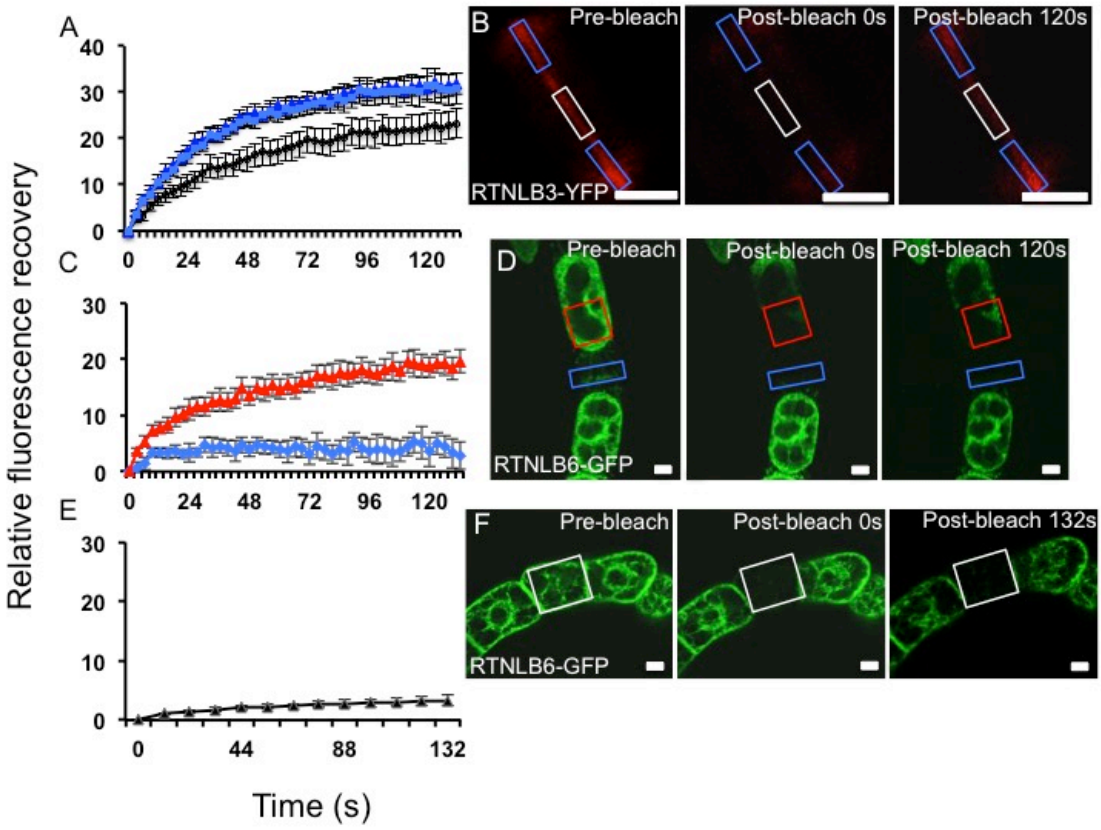

Figure 4
Fluorescence recovery after photobleaching (FRAP) reveals that RTNLB mobility is reduced in areas of PD development during cell plate formation.
A, FRAP comparing the leading edge of the developing cell plate (light and dark blue) with the centre of the cell plate (black diamonds) in BY2 cells expressing RTNLB3-YFP. **B** shows representative pre- and post-bleach images. Boxes indicate the bleached regions. **C**, RTNLB6-GFP on the ER associated with the primary PD at the cell wall in plasmolysed BY2 cells is immobile (blue diamonds), whereas within the protoplast, fluorescence recovers (red triangles) indicating RTNLB6-GFP mobility. **D** shows representative pre- and post-bleach images of RTNLB6-GFP labelled plasmolysed BY2 cells. Boxes indicate the bleached regions. **E**, whole cells bleached within a chain show that RTNLBs are not mobile between cells. **F** shows representative pre- and post-bleach images of RTNLB6-GFP labelled BY2 cells. Boxes indicate the bleached cell. Data are averages of at least 9 separate experiments and bars indicate standard error of the mean (SEM). Bars = 5 µm.

Figure 5

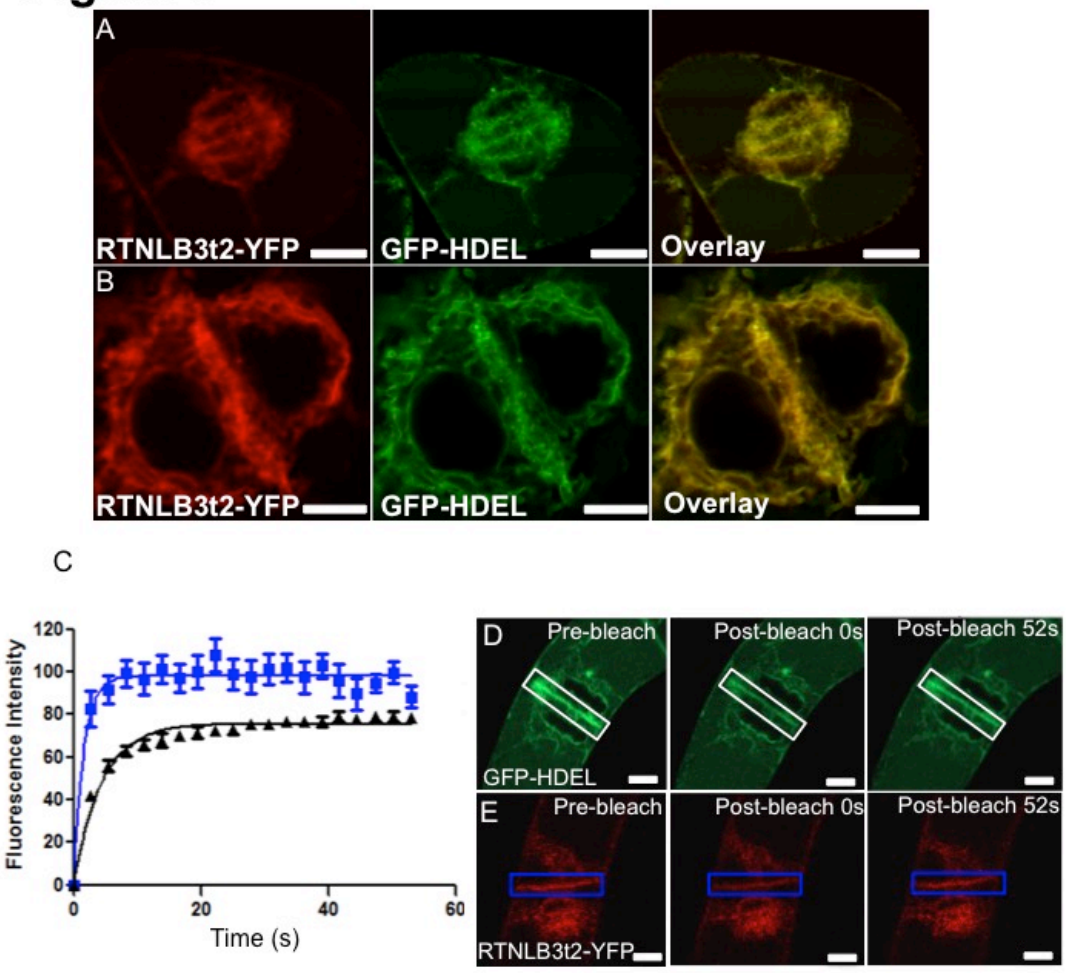

Figure 5
A truncated version of RTNLB3 (RTNLB3t2) is not recruited to the cell plate. **A** and **B** show RTNLB3t2-YFP co-expressed with GFP-HDEL. The overlaid images show that the RTNLB3t2 has even distribution across the ER, identical to GFP-HDEL, with no specific recruitment to the cell plate. **C**, FRAP of the cell plate in cells expressing RTNLB3t2-YFP showing that fluorescence recovers rapidly in the cell plate compared to GFP-HDEL and intact RTNLB3 (**D**, c.f. Fig.4 **A**). **D** and **E** represent pre- and post-bleach images. Bars = 5 μm.

Figure 6

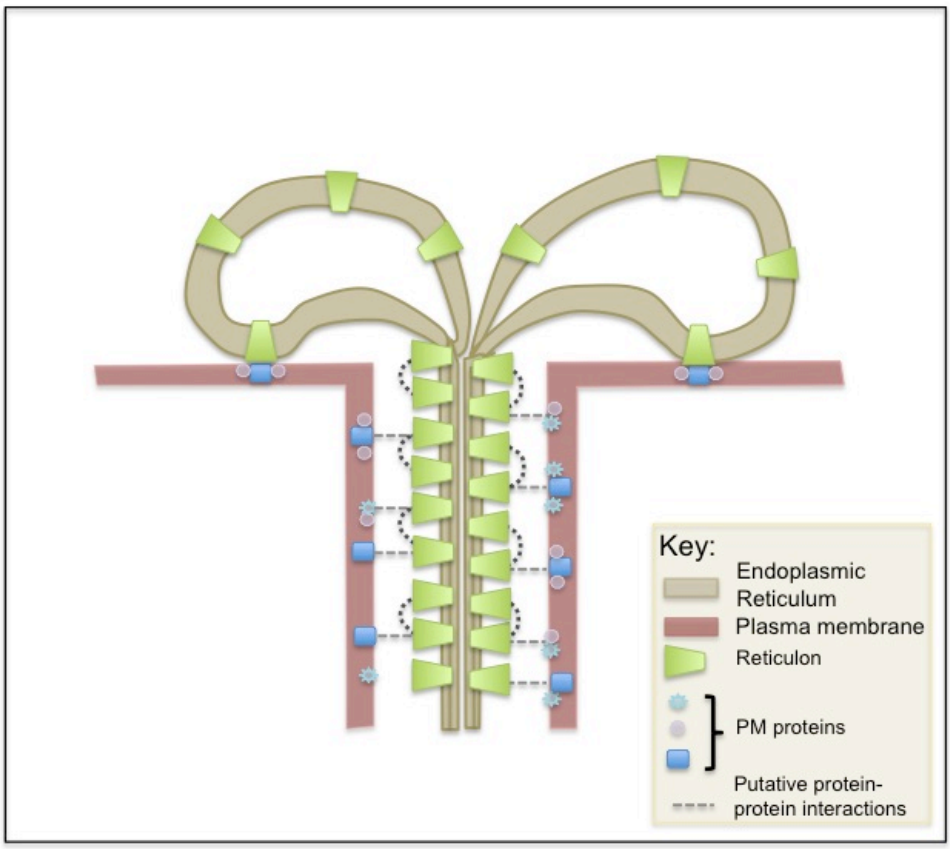

Figure 6
Model showing the insertion of RTNLB proteins into the membranes of the desmotubule. Putative protein-protein interactions between RTNLBs and proteins resident in the plasma membrane are depicted as broken lines.

Figure S1

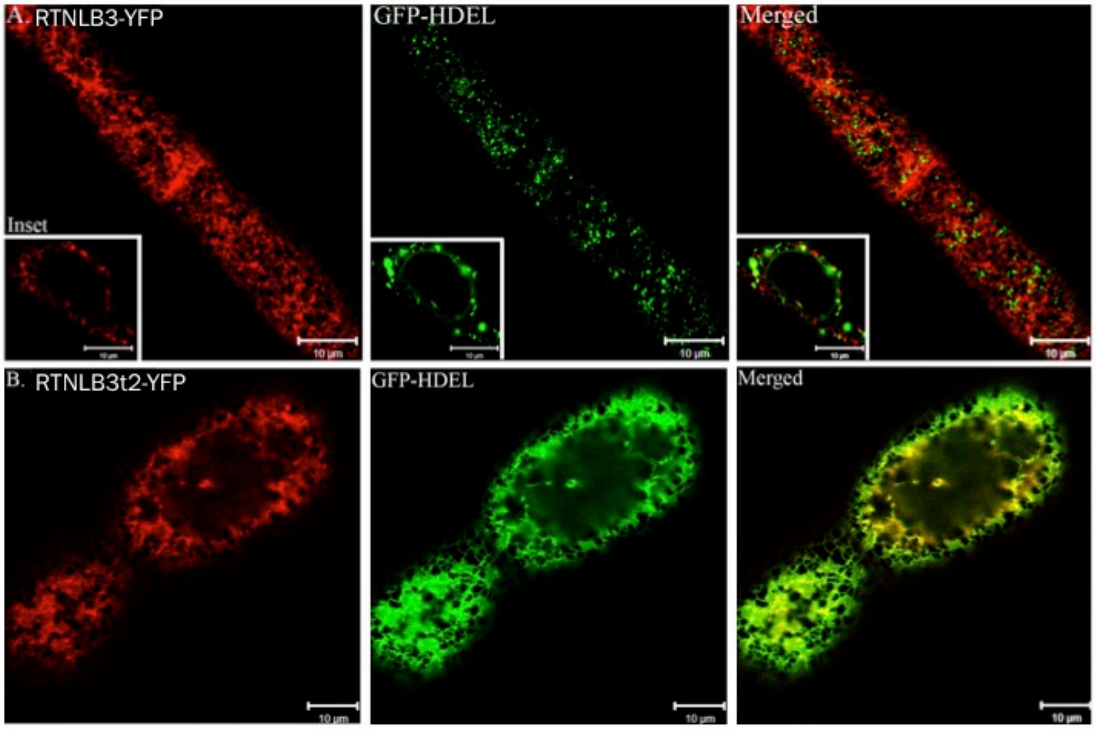

Supplementary Figure 1

RTNLB3-YFP can constrict the ER in interphase BY2 cells, whilst a truncated version cannot. A) GFP-HDEL is squeezed from the ER lumen into discrete lumenal pockets when co-expressed with RTNLB3-YFP. Inset shows the nuclear envelope which has a low degree of curvature and is not labelled by RTNLB3. B) RTN3t2-YFP co-expressed with GFP-HDEL does not constrict the ER in BY2 cells.

Figure S2

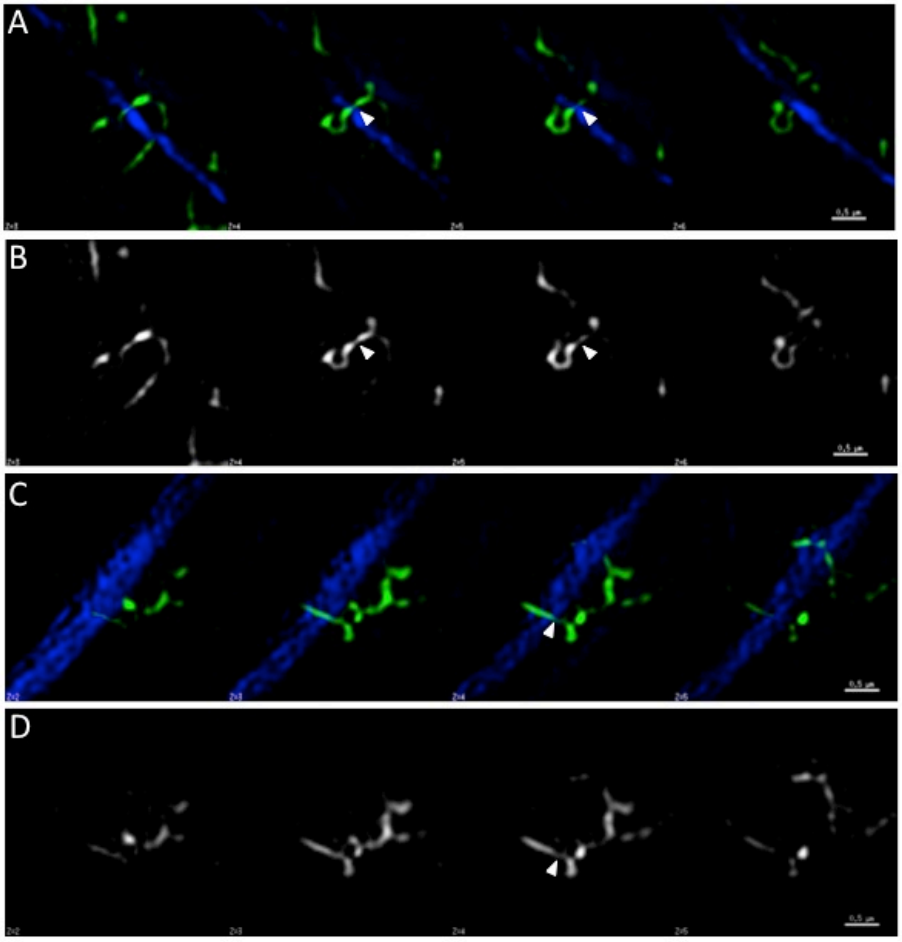

Supplementary Figure 2

RTNLB6-GFP labels desmotubules in BY2 cells. Optical sections taken 150 nm apart in the axial dimension, show that a single desmotubule can be tracked as it crosses the cell wall. A and C) Series of sections showing RTNLB6-GFP (green) labelled ER is highly constricted as it passes through the cell wall (blue) B) Single channel of images in A or C, showing RTNLB6-GFP only. Bars = 0.5 µm.

Supplementary Video 1

Movie depicting a 3D reconstruction of ER (labelled with RTNLB6-GFP) associated with PD in BY2 cells. Desmotubules can be seen as highly constricted regions crossing through the cell wall.